RSC Advances

This is an *Accepted Manuscript*, which has been through the Royal Society of Chemistry peer review process and has been accepted for publication.

Accepted Manuscripts are published online shortly after acceptance, before technical editing, formatting and proof reading. Using this free service, authors can make their results available to the community, in citable form, before we publish the edited article. This *Accepted Manuscript* will be replaced by the edited, formatted and paginated article as soon as this is available.

You can find more information about *Accepted Manuscripts* in the **Information for Authors**.

RSC Advances

RSCPublishing

ARTICLE

A study of nanogels with different polysiloxane chain lengths for photopolymerization stress reduction and modification of polymer networks properties

Cong Chen,[a,b] Minglei Li,[b] Yanjing Gao,[b] Jun Nie,[a,b] and Fang Sun[a,b]* ,

This paper reports a series of nanogel compositions synthesized with methacrylate-modified polysiloxanes of different chain lengths, urethane dimethacrylate (UDMA) and isobornyl methacrylate (IBMA) at molar ratios of 10:20:70 in the presence of a thiol chain transfer agent. The nanogel structures were characterized by proton nuclear magnetic resonance (^{1}H-NMR), Fourier transform-infrared spectroscopy (FT-IR), gel permeation chromatography (GPC) and transmission electron microscopy (TEM). From simultaneous measurement of real-time kinetics and shrinkage stress during photopolymerization, the nanogel additives showed a significant delay in the onset of stress and further reduce overall photopolymerization stress without compromising mechanical properties of the corresponding polymers. Most importantly, it is also proved that thermostability, flexibility and hydrophobic properties were improved by the introducing polysiloxane-based nanogels into UV-curable materials due to high temperature resistance, excellent flexibility and low surface energy associated with the polysiloxane component.

Introduction

Photopolymerization technique is one of the fastest developed environmental friendly polymerization technology because of its distinct advantages such as solvent-free formulations, low energy consumption, room temperature treatment, high efficiency, and spatial and temporal control.[1,2] Accordingly, photopolymerization materials have been extensively used in many areas including coating[3,4], adhesive[5], printing ink[6], dental materials[7] and stereolithography (SLA)[8]. However, volumetric shrinkage and shrinkage stress in the polymerization process,[9] which contribute to internal and interfacial defects, warped structures as well as inferior mechanical properties,[10] remain as critical problems for a wide array of polymeric materials applications,[11] especially for SLA that is the first commercialized method of 3D printing technology, due to friendly environment, high resolution (25 μm layers) and energy efficiency (1.5 cm/h building speed).[12] In addition, drawbacks of photopolymerization resins involving fragility, moisture absorption, and poor resistance to heat and corrosion, also are not negligible. Thus, reduction of shrinkage stress and further improvement of properties for photopolymerization materials have attracted much attention in recent years.

At present, various strategies have been applied in reducing shrinkage stress, involving changes in monomer structure or chemistry[13], addition of fillers or additives[14], and changing process condition[15]. In recent studies, reactive nanogel with high molecular weight additives of approximately 10 nm in dimension can be used as a practical and generic means to achieve substantial reductions in polymerization shrinkage and shrinkage stress in common polymers[16-18]. The addition of the nanogels to polymerization systems can also help improve the mechanical performances of the final polymer network through physical entanglement as well as covalent cross-linking between nanogels and the resin matrix. Nanogels, hyperbranched polymeric nanoparticles, have versatile structures, large number of chain ends and the ability to incorporate stimuli-responsive functionalities[19]. They have been widely researched and applied in the fields of drug delivery[20], dental materials[21], tissue engineering[22], photonic materials[23], modifiers for coatings and polymer composites[24]. To further expand application areas of nanogels, effort to design and develop functional nanogels remains the current research focus. The particular molecular structure of polysiloxane endows it with many unique properties, for example, low surface tension, resistance to wide range of temperatures, excellent flexibility and chemical inertness[25-27]. This stimulated our interest in introducing polysiloxane into nanogels to enhance the flexibility, resistance to high temperature and moisture absorption of photopolymerization materials. The polysiloxane-based nanogels would be expected to have a potential application in photopolymerization materials and 3D printing technology.

In the current study, a series of nanogel compositions were synthesized based on methacrylate-modified polysiloxanes with different chain lengths, urethane dimethacrylate (UDMA) and isobornyl methacrylate (IBMA) at molar ratios of 10:20:70. We also synthesized a nanogel without polysiloxane as a reference. Formulations were prepared by dispersing the nanogels into a dimethacrylate monomer at 10 wt% nanogel loading concentrations with a variety of properties evaluated including photopolymerization kinetics and shrinkage stress. The physical

and mechanical properties, thermal properties, and water absorption of UV-cured films containing polysiloxane-based nanogels were also studied.

Experimental details

Materials and characterization

Dual-end terminated methacrylate-modified polysiloxanes (M-Si-S/M/L) (M_n=380/900/1760, methacrylate equivalent: 190/450/880 g mol^{-1}, respectively) were donated by Shin-Etsu Chemical Co. Ltd. (Shanghai, China). Isobornyl methacrylate (IBMA) and triethylene glycol dimethacrylate (TEGDMA) were donated by Eternal Chemical Co. Ltd. (Zhuhai, China). Urethane dimethacrylate (UDMA) and 2-isocyanatoethyl methacrylate (IEM) were purchased from Heowns Business License Co. Ltd. (Tianjin, China). 2-Mercaptoethanol (ME) was supplied by Fuchen Chemical Reagents Factory (Tianjin, China). Azobisisobutyronitrile (AIBN) was purchased from Xilong Chemical Co. Ltd. (Shantou, China). 2,2-Dimethoxy-2-phenylacetophenone (DMPA) was obtained from Ciba Geigy Co. Dibutyltin dilaurate (DBTDL) was supplied by Shanghai Chemical Reagents Co. (Shanghai, China). Ethyl acetate, hexane, methanol and dichloromethane (DCM) were purchased from Beijing Chemical Works (Beijing, China). All reagents were used as received without further purification. The structures of the main reagents used are shown in Fig. S1.

Nuclear magnetic resonance (NMR) spectra were recorded using a Bruker AV400 unity spectrometer (resonance frequency of 400 MHz for proton). CDCl$_3$ was used as solvent.

The fouriertransform infrared (FT-IR) spectra (scanned between 400 and 4000 cm^{-1}) were obtained using a Nicolet 50XC spectrometer (Nicolet, USA).

Gel permeation chromatography (GPC) was performed to determine the molecular weight (Mw) and polydispersity (PDI) of the nanogels using a Waters 515-2410 GPC system with tetrahydrofuran (1.0 mL min^{-1}) used as the mobile phase.

The average size and size distribution of the nanogels were measured by dynamic light scattering (DLS) using a Zetasizer NanoZS (ZEN 3600, Malvern,Germany). All measurements were carried out at 25 °C using a 633 nm wavelength beam at 90° scattering angle.

Transmission electron microscopy (TEM) images were obtained with JEOL JEM-2010 high resolution transmission electron microscopes. The accelerating voltage was 20.0 kV.

The viscosity of the nanogel-modified TEGDMA resins was measured at 15 °C using NDJ-5S viscometer (Shanghai Changji Instrument Co. Ltd, China). Three replicates were conducted for each sample.

Dynamic mechanical thermal analyses (DMTA) were performed on DMTA-IV (Rheometric Scientific Co.) with samples which underwent post-cure conditioning at 160 °C overnight to fully cure, were run from -50 to +250 °C at a heating rate of 5 °C min^{-1} with a frequency of 1 Hz.

The tensile properties of cured films were measured with a material testing instrument (Instron-1211) at 25 °C. The rate of extension was 10 mm/min.

Thermogravimetry analysis (TG) curves were obtained on a STA-449C simultaneous thermogravimetric analyzer (Netzsch) under nitrogen with a flowing rate of 30 mL/min in the temperature range 30-500 °C with a heating rate of 10 °C min^{-1}.

Synthesis of polysiloxane-based nanogels

M-Si-S/M/L, UDMA and IBMA at molar ratios of 10:20:70 were used to synthesize polysiloxane-based nanogels. Synthesis details and operation methods are similar to previous publications[16,17].The difference is that the resulting clear nanogel reaction mixture was added drop-wise to an eight-fold excess of hexanes (for Si10S) or methanol (for Si10M and Si10L) to precipitate the polymeric materials. The final polysiloxane-based nanogels are designated as Si10S, Si10M and Si10L, respectively, to represent the 10 mol% component and different polysiloxane chain lengths in the nanogels. The yields of three nanogels are approximately 85 %, 81 % and 77 %, respectively. Similarly, a nanogel (UI) without polysiloxane was synthesized based on UDMA and IBMA at molar ratios of 30:70 in the same procedures as a reference. The characterizations of UI were shown in Fig. S2-S3.

IR spectra and ^{1}H-NMR spectra of Si10S/M/L display the following similar characteristics:

IR (KBr, cm^{-1}): 3200-3500 cm^{-1} (-NH), 2925-2975 cm^{-1} (-CH$_3$, -CH$_2$), 1725 cm^{-1} (>C=O), 1639 cm^{-1} (-C=CH-), 1260 cm^{-1} (Si-CH$_3$), 1020-1092 cm^{-1} (Si-O-Si), 800-804 cm^{-1} (Si-CH$_3$). (Fig. S4-S6)

^{1}H-NMR (400MHz, CDCl$_3$, ppm): δ5.6-6.2 (-C=CH$_2$), δ4.0-4.6 (-CH$_2$CH$_2$-O-), δ2.8-3.5 (-NH-), δ1.7-2.0 (H$_2$C=C-CH$_3$), δ0.53-1.68 (-Si-CH$_2$-), δ0.05-0.10 (-Si-CH$_3$). (Fig. S7-S9)

^{29}Si NMR (CDCl$_3$, ppm): 10.00 (-CH$_2$-Si(CH$_3$)$_2$-O-), -21.96 (-O-Si(CH$_3$)$_2$-O-). (Fig. S10)

GPC (Multiple PS standards) for Si10S/M/L: Mn=110,000, 400,000 and 667,000; PDI (polydispersity) =2.11, 4.16 and 7.89, respectively.

Preparation of polymer films containing the nanogels under anaerobic conditions

The liquid UV-curable samples that consisted of the different nanogels and TEGDMA in mass ratios of 10 wt% were prepared. DMPA (0.5 wt%, relative to resin) was added to each sample as a photoinitiator. The samples were mechanically agitated until the nanogels were fully dispersed to give optically clear monomeric solutions. Then a measured volume of the liquid UV-curable samples was dispensed on a pre-cleaned glass slide and allowed to spread to a diameter of 20 mm to obtain liquid resin film of the thickness of 0.3 mm. A coverglass was then placed over the film to ensure anaerobic conditions. Subsequently, the liquid resin film was exposed to the high-pressure mercury lamp (incident light intensity = 5 mW cm^{-2}, recorded by UV radiometer (Photoelectric Instrument Factory)) for 60 s to obtain the polymer film for evaluating a series of properties.

Simultaneous measurement of shrinkage stress and conversion

The dynamic shrinkage stress was evaluated for nanogel-modified TEGDMA formulations with a cantilever beam-based tensometer (Paffenbarger Research Center, American Dental Association). Instrument details and operation methods are provided in other publications[28]. The simultaneous rea-ltime NIR based conversion data during polymerization was collected in direct transmission mode via fiber optic cables. The decrease

of the methacrylate $=CH_2$ group absorption peak at 6165 cm^{-1} in the near-IR range accurately reflects the extent of the polymerization since the change of the absorption peak area is directly proportional to the number of the (meth-) acrylate double bond. Three replicates were carried out for each material composition.

Flexural strength test

Flexural strength tests for all materials were performed using bar specimens with dimensions of $15 \times 2 \times 2$ mm. Samples were photopolymerized between glass slides in an elastomer mold by exposure to UV light at 15 mW cm^{-2} for 10 min. The flexural strength and flexural modulus were obtained in three points bending on the MTS testing machine using a span of 10 mm and a cross-head speed of 1 mm min^{-1}.

Calculation of gel yield and water absorption

Gel yield is expressed as:

$$\text{Gel yield} = W_1/W_0 \times 100\% \quad (1)$$

where W_0 is the weight of liquid film before curing, W_1 is the weight of cured film which was obtained by extracting by ethanol for 24 h and drying to constant weight after irradiating the liquid film under UV lamp for 60 s. Three replicates were conducted for each sample.

Water absorption is expressed as:

$$\text{Water absorption} = (W_3 - W_2)/W_2 \times 100\% \quad (2)$$

where W_2 is the weight of UV-cured film before being soaked in deionized water, W_3 is the weight of UV-cured film after being soaked in deionized water at room temperature for 24 h. Three replicates were conducted for each sample.

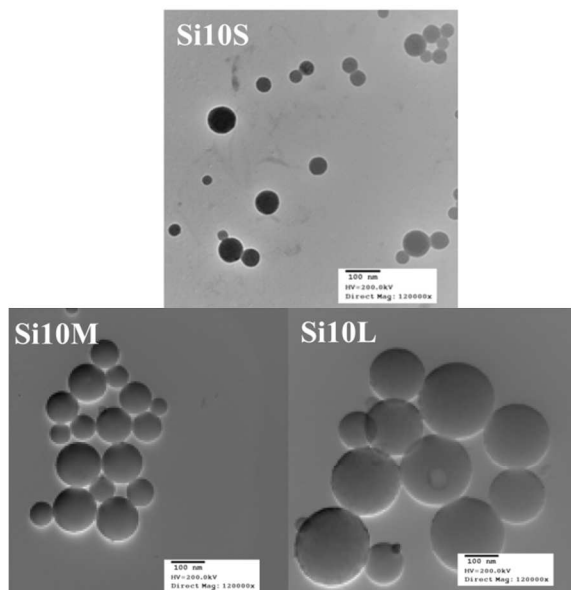## Results and discussion

Morphology of the Nanogels

Fig. 1 Transmission electron micrographs of Si10S/M/L.

The fact that all the nanogels appeared microspherical was full demonstrated in the TEM images of Si10S/M/L (Fig. 1) and the average diameters of Si10S/M/L were 52.9 nm, 64.5 nm and 122.6 nm, respectively. The average diameters of these nanogels are 59.6 nm for Si10S, 70.9 nm for Si10M and 128.2 nm for Si10L from DLS measurement. The average diameters from TEM are slightly smaller than those measured by DLS, which may be attributed to the transition of the assemblies from the swollen (DLS) to dried state (TEM). Furthermore, the increasing trend of the average diameters along with the increase of polysiloxane chain length was probably ascribed to the increase of the molecular weight of polysiloxane.
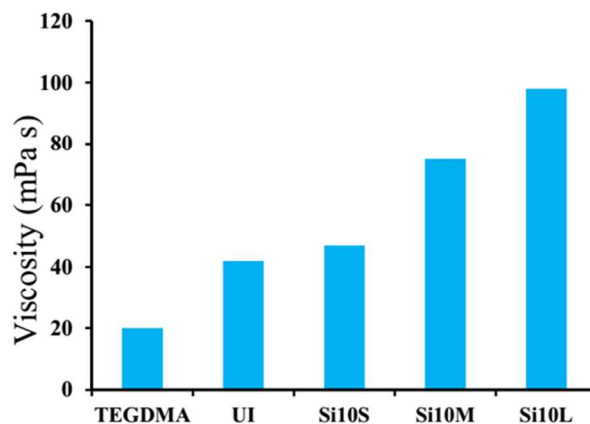
Viscosity

Fig. 2 Viscosity of UI and Si10S/M/L added into TEGDMA at 10 wt%.

Viscosity, one of the most important parameters, directly affects the flow ability of formulations and the rate of photopolymerization of formulations as well as the properties of cured films. Usually, viscosity is closely related to molecular weight, intermolecular chain entanglement and inter-/intramolecular hydrogen bond. A series of formulations, in which various nanogels were added to TEGDMA at 10 wt%, were prepared and their viscosities were measured, as shown in Fig. 2. The viscosity of TEGDMA, as control, was 20 mPa s. When the nanogels were loaded into TEGDMA, two phases were presented: a bulk TEGDMA phase and a nanogel phase that was infiltrated by the monomer. The friction force between nanogel and TEGDMA molecules as well as chains of the nanogel molecules leads to a higher viscosity environment in the interior and interfacial regions of the nanogel phase. Although at low loading levels, the effect of the dispersed nanogel on TEGDMA viscosity is minimal, the viscosity was increased to some extend with the addition of nanogels. Furthermore, the viscosity of formulation for Si10S was 47 mPa s, while the viscosity for Si10L was increased to 98 mPa s. This result was related to the increase of the size, volume fraction and molecular weight of the nanogels because the friction force and interfacial regions between the molecules may increase with the increase of the size, volume fraction and

molecular weight of nanogels, thereby leading to a high viscosity.

Photopolymerization kinetics

The final degree of double bond conversion (DC) and the rate of polymerization (Rp), as the most significant parameters characterizing the photopolymerization kinetics, were investigated by real-time infrared spectroscopy (RT-IR), as shown in Fig. 3 and Fig. 4. The unmodified TEGDMA control reached about 82% conversion after 10 min of irradiation and the Rp presented the typical early stage auto-acceleration with a rate maximum that occurred at approximately 52% conversion, as characteristic for low viscosity network-forming monomers. With the addition of nanogels, photopolymerization kinetics profiles and polymerization rate profiles for nanogel-modified materials were similar to the control. The final double bond conversions slightly increased with the increase of polysiloxane chain length. The conversions at the maximum rate of polymerization were decreased with the increase of polysiloxane chain length, and they were higher than TEGDMA but lower than UI. The difference may be related to the fact that with the addition of nanogels, the interior and interfacial regions of the nanogel phase presented a high viscosity environment to produce the more mobility-restricted state, leading that the overall auto-acceleration behaviour would vary accordingly.[29]
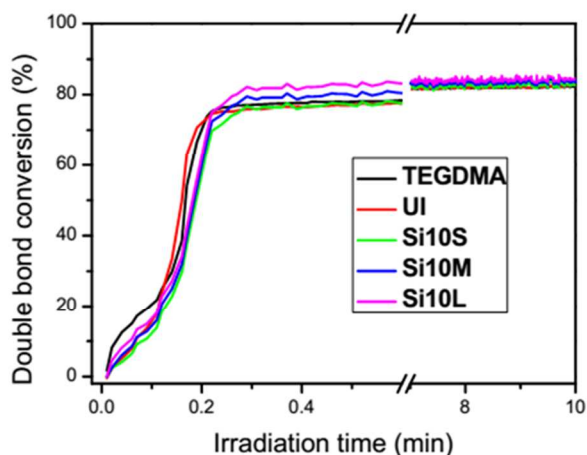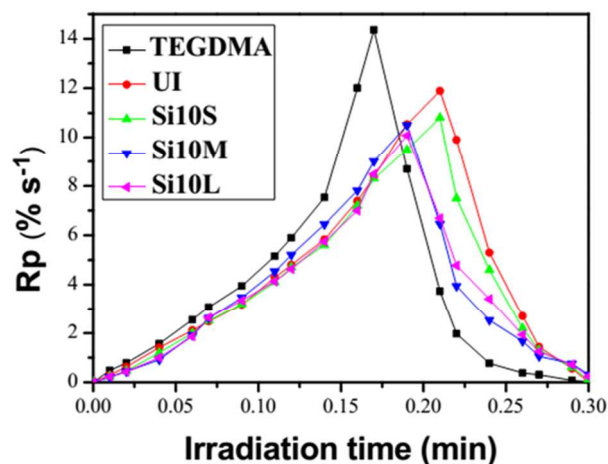

Fig. 4 Polymerization rate profiles for the control, UI and Si10L/M/H nanogel-modified materials at 10 wt%.

Shrinkage stress in photopolymerization

During polymerization, the bulk volume shrinkage and shrinkage stress are unavoidable due to the formation of new covalent bonds formation, which remain as critical problems for a wide array of polymeric materials applications, particularly for vinyl-based glassy networks formed by a chain-growth mechanism that involves early gelation. As shown in Fig. 5, the baseline stress value of UV-cured TEGDMA control was about 2 MPa. With the addition of nanogels to TEGDMA monomer, the final shrinkage stress was markedly decreased compared with the control. This is related to the replacement of the monomer by the prepolymerized nanogel, which contributes to reduced overall reactive group concentrations and decreased volume change during the network formation. However, the increase of polysiloxane chain length of the nanogel negatively affected the final stress reduction due to the fact that long chain polysiloxane-based nanogel with high molecular weight may make its interior and interfacial regions present a high viscosity environment, which produces the more mobility-restricted state, thereby leading to early reaching gel point. In general, it can be expected that a higher conversion at the gel point leads to less shrinkage stress in the final material.
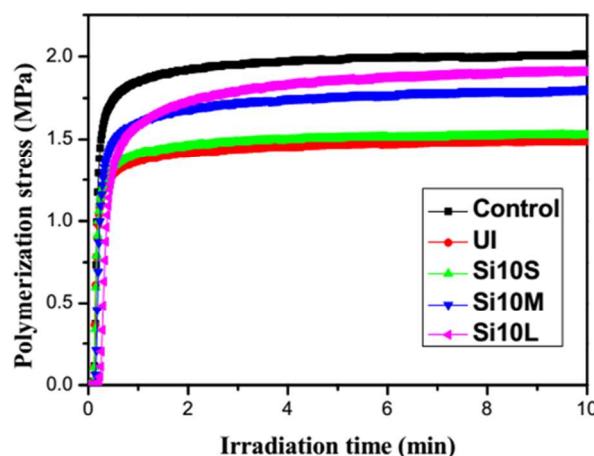

Fig. 3 Photopolymerization kinetics profiles for the TEGDMA, UI and Si10S/M/L nanogel-modified materials at 10 wt%.

Fig. 5 Shrinkage stress profiles for TEGDMA monomer and the materials containing 10 wt % nanogel.
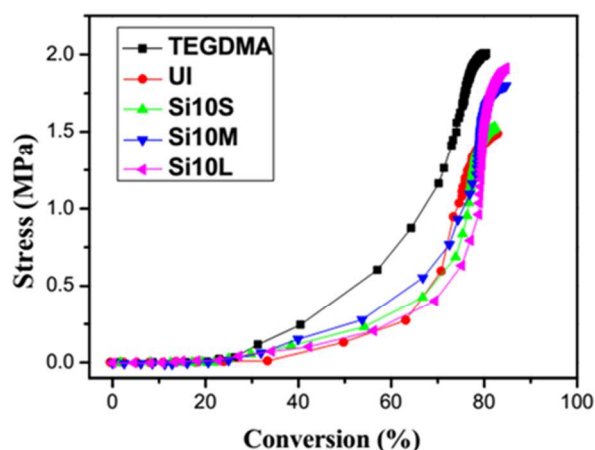

Fig. 6 Stress correlation with conversion for 10 wt% loading of nanogels in TEGDMA.

In order to further investigate the important role of the nanogel on the final stress value, the plots of polymerization stress vs. conversion were shown in Fig. 6. It was evident that the nanogel-based photopolymerization produced a significant delay in the onset of stress compared to the control. The delay in the onset of stress development as well as the point at which rapid stress rise was observed, indicating that both macrogelation and bulk vitrification were suppressed as a consequence of the nanogel-based network formation strategy. There was no clear trend in the delayed gelation based on the polysiloxane chain length of the nanogel.

Flexural strength and flexural modulus of photopolymerization materials

Flexural strength is an important mechanical property of photopolymerization materials for wide applications, while the flexural modulus is a critical parameter in the evolution of polymerization stress. From the flexural strength tests (Table 1), it was found that the TEGDMA control had a flexural strength of 78.6 MPa. It was obvious that by adding 10 wt% UI, Si10S and Si10M into the resin, the flexural strength was effectively maintained or even slightly improved compared with the TEGDMA control. This is because the addition of the nanogels with methacrylate groups that can serve as a cross-linking agent during photopolymerization increased the degree of cross-linking of the material. However, when Si10L was added, the flexural strength dramatically reduced to about 54.7 MPa, which may be related to the relatively low compatibility compared with Si10S and Si10M. A similar trend was observed in the flexural modulus results with the addition of different nanogels.

Table 1 Flexural strength and flexural modulus tests for UV-cured films.

Item	TEGDMA	UI	Si10S	Si10M	Si10L
Flexural strength (MPa)	78.6±6.8	74.9±5.7	78.1±5.5	83.9±6.1	54.7±4.3
Flexural modulus (GPa)	1.84±0.11	1.83±0.09	2.18±0.13	2.07±0.14	1.53±0.06

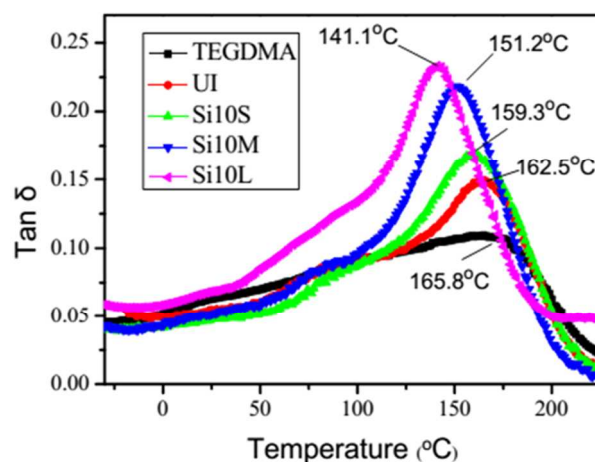### Dynamical mechanical thermal analyses of UV-cured films

Fig. 7 Tan δ behaviour for UV-cured films using a 10 $^{\circ}$C min^{-1} scan rate.

The samples of UV-cured films were investigated by dynamic mechanical thermal analysis (DMTA) to analyse their mechanical properties. The tan δ curve is sensitive to structural changes that occur at the molecular level during aging. The peak in the tan δ curve is associated with the movement of small groups and chains of molecules within the polymer structure, all of which are initially frozen in. In addition, the temperature at which the tan δ peak occurs is commonly known as glass transition temperature (T_g), which is an effective indicator in determining the performance and potential implementation of the polymer network. For the TEGDMA control, a broad damping peak (T_g at 165.8 $^{\circ}$C) was observed in Fig. 7, indicating a very heterogeneous polymer in terms of structural crosslink density variations within the TEGDMA network. When the nanogel was introduced at 10 wt%, the UV-cured film of each system had only one damping peak, which suggests that the nanogels have relatively good compatibility with TEGDMA. Moreover, in comparison with the cured film containing UI nanogel, intensity of damping peaks of UV cured films containing polysiloxane-based nanogels was relatively high, and increased with the increase of the polysiloxane chain length, while the Tg presented a contrary trend (from 159.3 $^{\circ}$C for Si10S to 141.1 $^{\circ}$C for Si10L), which can be ascribed to the high flexibility or low T_g of the polysiloxane.
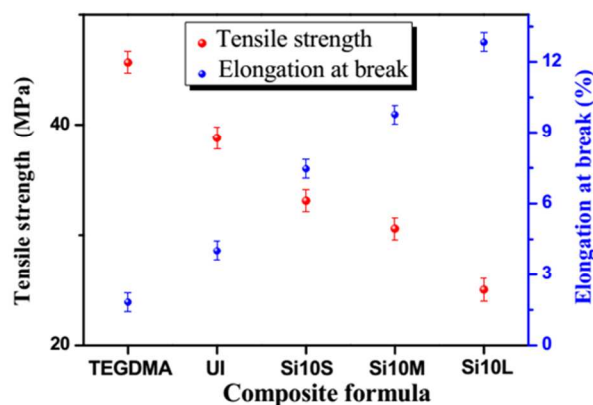
Tensile properties of UV-cured films

Fig. 8 Tensile strength and elongation at break of UV-cured films.

Fig. 9 (a) Water absorption of UV-cured films; (b) Gel yield of UV-cured films.

To further study the physical and mechanical properties of UV-cured films containing the nanogels, tensile properties were investigated as a vital indicator for the practical applications. As shown in Fig. 8, the tensile strength of the TEGDMA control was 45.7 MPa and its elongation at break was 1.82%. With the addition of nanogels, the tensile strength of the cured films was decreased and elongation at break was increased. The tensile strength of the cured films with polysiloxane-based nanogels was lower than that with UI nanogel, while elongation at break was higher. In addition, the cured films for polysiloxane-based nanogels presented a decreasing trend in the tensile strength and an increasing trend in the elongation at break with the increase of the chain length of polysiloxane. These results indicated that introducing the nanogel with flexible polysiloxane chains can enhance extensibility of cured films.

Water absorption and gel yield of UV-cured films

As shown in Fig. 9 (a), water absorption of TEGDMA control was 4.2%. When the nanogels were added to TEGDMA, the water absorption of cured films was decreased. And for cured film with UI nanogel, the water absorption was higher than that with polysiloxane-based nanogels. Moreover, the water absorption of cured films with polysiloxane-based nanogels slightly decreased from 3.5% for Si10S to 2.6% for Si10L along with the increase of polysiloxane chain length. From Fig. 9 (b), the gel yields increased with the increase of polysiloxane chain length. As such, it was proposed that the UV-cured films containing polysiloxane-based nanogels had compact and hydrophobic film surfaces because of the low surface tension of polysiloxane and high crosslinking densities of cured materials.
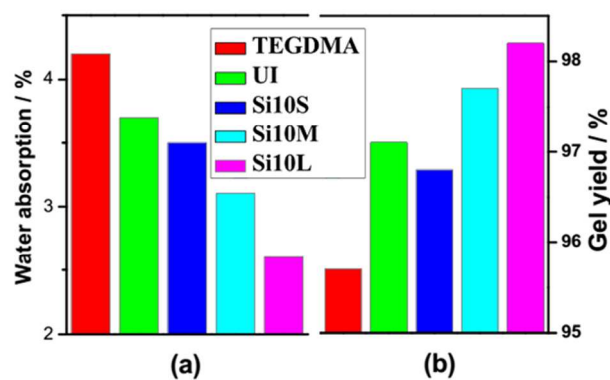
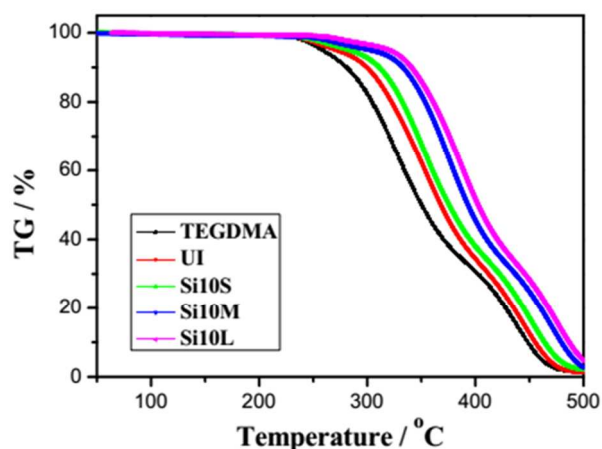### Thermogravimetric analysis of UV-curing films

Fig. 10 TG curves of UV-cured films.

The thermal stability of a polymer network is a very important property, investigated by thermogravimetric analysis under nitrogen atmosphere. Fig. 9 and Fig. 10 show the TG and DTG curves of UV-cured films, while detailed parameter values obtained from the TG and DTG curves are listed in Table 2. The thermal degradation processes of UV cured films underwent single-step degradations with three DTG peaks. The temperatures at the first DTG peak were close to $T_{5\%}$, which were attributed to the degradation of small molecules with low molecular weight. It can be easily found that T_{max1} and T_{max2} of the UV-cured films containing nanogels were higher than the TEGDMA control, indicating the addition of nanogels can improve the thermal stability of UV-cured films, because of the increase of the degree of cross-linking. Meanwhile, thermal stability of UV-cured films with UI nanogel was lower than that with polysiloxane-based nanogels. Furthermore, the thermal stability of the cured films containing the nanogel with long polysiloxane chain was improved. This was related to relatively high mass fraction of polysiloxane in the nanogel because the Si-O bond was stronger than C-C and C-O bonds.
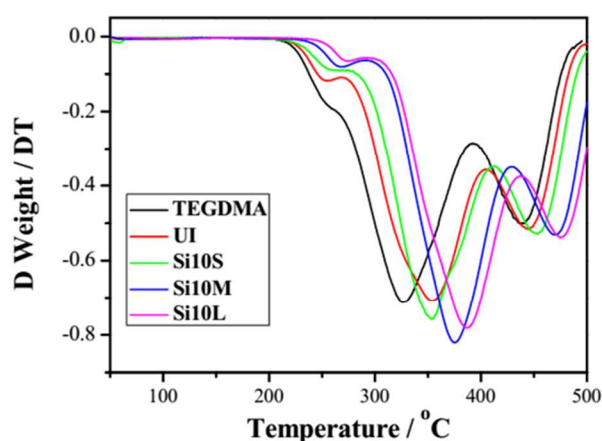
Fig. 11 DTG curves of UV-cured films.

Table 2 Thermal decomposition parameters of examined UV-cured films

UV-cured film	$T_{5\%}(^{o}C)$	$T_{max1}(^{o}C)$	$T_{max2}(^{o}C)$
TEGDMA	259	324	437
UI	271	353	444
Si10S	284	353	453
Si10M	304	375	470
Si10L	320	387	475

Note: $T_{5\%}$ is the temperature of 5% weight loss. T_{max} is the peak temperature at maximum weight loss rate.

Conclusions

In this paper, three kinds of nanogels with different polysiloxane chain lengths were synthesized and their structures were confirmed by FT-IR, ^{1}H-NMR, GPC and TEM. The nanogels were mixed with TEGDMA at 10 wt% loading level to evaluate a series of properties. The photopolymerization kinetics showed that the nanogel-modified systems exhibited satisfying photopolymerization efficiency. All investigated nanogel additives can produce a significant delay in the onset of stress to decrease photopolymerization stress without compromise to mechanical properties of the corresponding polymers. However, the increase of polysiloxane chain length of the nanogel negatively affected the final stress reduction. Most significantly, it is also proved that long chain polysiloxane-based nanogels can improve flexibility, thermostability and hydrophobicity of UV-curable materials. Thus, polysiloxane chain length is one of crucial factors affecting properties of polysiloxane-based nanogels. The polysiloxane-based nanogels have a potential application in photopolymerization materials and 3D printing technology.
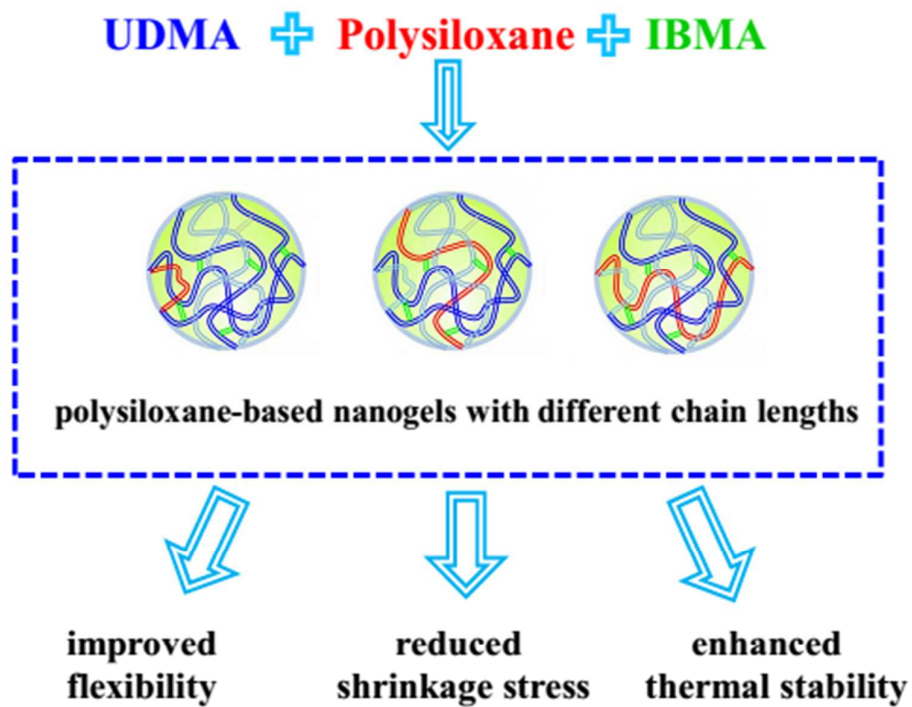
Acknowledgements

Notes and references

[a] State Key Laboratory of Chemical Resource Engineering, Beijing University of Chemical Technology, Beijing 100029, People's Republic of China.

[b] College of Science, Beijing University of Chemical Technology, Beijing 100029, People's Republic of China

1 Z. Tarle, A. Meniga, M. Ristic, J. Sutalo, G. Pichler and C. L. Davidson, *J. Oral Rehabil.*, 1998, **25**, 436-442.

2 R. P. Sebra, K. S. Anseth and C. N.Bowman, *J. Polym. Sci., Part A: Polym. Chem.*, 2006, **44**, 1404-1413.

3 K. Maag, W. Lenhard and H. Loffles, *Prog. Org. Coat.*, 2000, **1**, 93-97.

4 S.Sepeur, N. Kunze, B. Werner and H. Schmidt, *Thin Solid Films*, 1999, **351**, 216-219.

5 H. Christian, C. Souleymane, R. Anita, L. F. Gina and W. Christoph, *Appl. Mater. Interfaces*, 2014, **6**, 4713-4719.

6 D. Cathal, O'Connell; J. H. Michael, M. David, E. M. Simon and G. W. Gordon, *Langmuir*, 2014, **30**, 2712-2721.

7 S. G. Pereira, T. G. Nunes and S. Kalachandra, *Biomaterials*, 2002, **23**, 3799-3806.

8 F. P. W. Melchels, J. Feijen and D. W. Grijpma, *Biomaterials*, 2010, **31**, 6121-6130.

9 J. W. Stansbury, M. Trujillo-Lemon, H. Lu, X. Z. Ding, Y. Lin and J. H. Ge, *Dent. Mater.*, 2005, **21**, 56-67.

10 S. Maruo and K. Ikuta, *Sens. Actuators, A: Phys.*, 2002, **100**, 70-76.

11 R. R. Moraes, J. W. Garcia, M. D. Barros, S. H. Lewis, C. S. Pfeifer, J. C. Liu and J. W. Stansbury, *Dent. Mater.*, 2011, **27**, 509-519.

12 B. C. Gross, J. L. Erkal, S. Y. Lockwood, C. Chen and D. M. Spence, *Anal. Chem.*, 2014, **86**, 3240-3253.

13 L.G. Lovell, L. Hui and C.N. Bowman, *Dent. Mater.*, 2001, **17**, 504-511.

14 J.D. Satterthwaite, K. Vogel and D.C. Watts, *Dent. Mater.*, 2009, **25**, 1612-1615.

15 J. Richeton, S. Ahzi, K.S. Vecchio and F.C. Jiang, *Int. J. Solids Struct.*, 2006, **43**, 2318-2335.

16 C. Chen, J. C. Liu, F. Sun and J. W. Stansbury, *RSC Adv.*, 2014, **4**, 28928-28936.

17 C. Chen, J. C. Liu, F. Sun and J. W. Stansbury, *J. Polym. Sci., Part A: Polym. Chem.*, 2014, **52**, 2830-2840.

18 J. Liu, I. Y. Rad, F. Sun and J. W. Stansbury, Polym. Chem., 2013, **5**, 227–233.

19 N. B. Graham and A. Cameron, *Pure Appl. Chem.*, 1998, **70**, 1271-1275.

20 M. H. Xiong, Y. Bao, X. J. Du, Z. B. Tan, Q. Jiang, H. X. Wang, Y. H. Zhu and J. Wang, *ACE Nano*, 2013, **7**, 10636-10645.

21 N. B. Cramer, J. W. Stansbury and C. N. Bowman, *J Dent Res*, 2011, **90**, 402-416.

22 V. Daniloska, P. Carretero, R. Tomovska, M. Paulis and J. M. Asua, *ACS Appl. Mater. Interfaces*, 2014, **6**, 3559-3567.

23 A. Doring, W. Birnbaum and D. Kuckling, *Chem. Soc. Rev.*, 2013, **42**, 7391-7420.

24 C. D. Donahoe, T. L. Cohen, W. L. Li, P. K. Nguyen, J. D. Fortner, R. D. Mitra and D. L. Elbert, *Langmuir*, 2013, **29**, 4128-4139.

25 G. N. Li, S. L. Jiang, Y. J. Gao, X. K. Liu and F. Sun, *Ind. Eng. Chem. Res.*, 2013, **52**, 2220-2227.

26 Y. Yu, B. Liao, G. N. Li, S. J. Jiang and F. Sun, *Ind. Eng. Chem. Res.*, 2014, **53**, 564-571.

27 F. Sun, X. K. Liu, L. Zhang and H. G. Du, *Ind. Eng. Chem. Res.*, 2012, **51**, 240-247.

28 H. Lu, J. W. Stansbury, S. H. Dickens, F. C. Eichmiller and C. N. Bowman, J. Biomed. *Mater. Res., Part B*, 2004, **71**, 206-213.

29 J. C. Liu, G. D. Howard, S. H. Lewis, M. D. Barros and J. W. Stansbury, *Eur. Polym. J.*, 2012, **48**, 1819-1828.

RSC Advances Accepted Accepted Manuscript

UDMA + Polysiloxane + IBMA

polysiloxane-based nanogels with different chain lengths

improved
flexibility

reduced
shrinkage stress

enhanced
thermal stability

The polysiloxane-based nanogels with different chain lengths can not only reduce polymerization stress, but also improve the flexibility, thermostability and hydrophobic property of photopolymerization materials.